PERGAMON

International Journal of Solids and Structures 38 (2001) 5625–5645

INTERNATIONAL JOURNAL OF SOLIDS and STRUCTURES

www.elsevier.com/locate/ijsolstr

Adaptive multilayer perceptron networks for detection of cracks in anisotropic laminated plates

Y.G. Xu, G.R. Liu *, Z.P. Wu, X.M. Huang

Department of Mechanical and Production Engineering, Center for Advanced Computations in Engineering Science (ACES), National University of Singapore, 10 Kent Ridge Crescent, Singapore 119260, Singapore

Received 18 April 2000; in revised form 9 October 2000

Abstract

In this study, an adaptive multiplayer perceptron (MLP) technique is proposed for the detection of cracks in anisotropic laminated plates. The displacement response on the surface of plate, excited by a time-harmonic line load, is used as the input of the MLP. The crack parameters that specify the location and size of the cracks in the anisotropic laminated plates are taken as the output of the MLP. The MLP model is first trained to establish the nonlinear relationship between the scattered surface displacement response and the corresponding location and size of the cracks. The scattered displacement responses required in training samples are calculated from the strip element method (SEM). To facilitate this training process, the correlation analysis for the outputs of neurons in the hidden layers of the MLP model is carried out to optimize the MLP architecture. A modified back-propagation learning algorithm with a dynamically adjusted learning rate and an additional jump factor is developed to speed up the convergence of the MLP model in the training process. The concept of orthogonal array is adopted to generate the representative combinations of the crack parameters, which significantly reduces the number of samples while maintaining the completeness of sample data. The well-trained model is then used to reconstruct the crack parameters by feeding in the measured displacement response on the plate surface. These reconstructed crack parameters are further examined by comparing their resulting displacement response from the SEM forward calculation with the measured displacement response. If the comparison is satisfactory, the reconstructed crack parameters would be considered to be true and the computation ends. Otherwise, the MLP model would go another round of re-training process until the satisfactory reconstruction is obtained. The proposed technique was verified numerically using an anisotropic laminated plate $[C0/G+45/G–45]_s$ with four types of horizontal cracks. The verification includes the detection for both the location and the size of cracks using the simulated response data with and without noise.

Keywords: Neural networks; Composite materials; Damage detection; Elastic waves

1. Introduction

With the increasing application of the composite materials in aircraft, aerospace, mechanical engineering, civil engineering, etc., detection of cracks or flaws in composite materials has become more and

* Corresponding author. Tel.: +65-874-6481; fax: +65-874-4795/+65-779-1459.
E-mail address: mpeliugr@nus.edu.sg (G.R. Liu).

0020-7683/01/$ - see front matter
PII: S0020-7683(00)00368-1

more important. Although conventional ultrasonic techniques, such as ultrasonic B- and C-scan techniques, have been widely used for this purpose and also obtained a reasonable amount of success, difficulties still remain for various types of the practical applications. The reason is that these conventional techniques are based on the real-time measurements of reflected or transmitted pulses from the incident body waves such as longitudinal waves. Very often, these measured pulse signals are not sufficient enough to provide the clear image of the cracks or flaws due to either the inhomogeneous nature of materials or too many wave reflections generated by the different laminate interfaces in the composite plate.

In order to overcome the difficulties associated with the ultrasonic wave reflection, many new detection techniques have been developed recently (Karim and Kundu, 1989, 1990; Karim et al., 1989; Liu and Lam, 1994; Doebling et al., 1996; Luo and Hanagud, 1997). One of them is to infer the location and size of cracks from the elastic low-frequency waves scattered by these cracks or flaws (Liu and Achenbach, 1994, 1995; Liu and Lam, 1994; Liu et al., 1995, 1996). This technique actually originates from the investigation on the waves scattered by the cracks or flaws hidden inside the laminates. Much work of this kind investigation has been done so far. For examples, Karim and Kundu (1989), Karim et al. (1989, 1992a,b) studied the scattering of elastic waves due to cracks and flaws in plates using the combination of finite element method (FEM) and the guided wave expansions. Kundu and Hassan (1987) and Kundu (1988) investigated the dynamic interaction between two interface cracks and the transient behavior of an interfacial crack in composite plates. Karunasena et al. (1991) calculated the scattering of the plane-strain waves due to the cracks using the combined FEM and Lamb wave modal expansion method. Liu et al. (1991) studied the transient scattering of Rayleigh Lamb waves of a surface-breaking crack using the FEM and boundary element method (BEM). Their calculated results were also compared with the measured ones. Datta et al. (1992) and Liu and Datta (1993) later applied the similar method to investigate the scattering of both impact and ultrasonic waves due to the cracks in a composite plate. In order to improve the computational efficiency, Liu and Lam (1994), Liu and Achenbach (1994, 1995), Liu et al. (1995, 1996), Lam et al. (1997) and Wang et al. (1998) used a strip element method (SEM) to investigate both horizontal and vertical cracks in the composite laminated plates subjected to the moving or fixed source loads. The numerical analysis were carried out in both time and frequency domains, and the calculated results were compared with the ones in noncrack cases. All these works demonstrated that the scattered elastic waves are significantly related to the location and size of cracks or flaws, but these studies can not be directly employed for the detection of cracks or flaws from the scattered waves. This is because that analysis for the scattered waves with the given crack or flaw configuration is referred to the forward solution, while the detection for the cracks or flaws from the scattered waves is referred to an inverse problem. The inversion for this kind of problems is mathematically nonlinear, analytically intractable and hence not easy. So the established detection technique based on the scattered waves is not yet available, although there are some polynomial formulae proposed so far for approximately estimating the larger cracks in laminated plates (Liu and Lam, 1994; Lam et al., 1997).

With the developments of artificial intelligent techniques, neural networks (NN) have provided an effective tool for solving this kind of inverse problems. Indeed, there is an increasing interest in employing the NN techniques to detect structural damages in recent years. Wu et al. (1992) adopted an NN model to portray the structural behavior before and after damage in terms of the frequency response function, and then used this trained model to detect the location and extent of damages by feeding in measured dynamic response. Klenke and Paez (1994) used two probabilistic techniques to detect the damages in the aerospace housing components, one of which involved a probabilistic NN model. Rhim and Lee (1995) used the MLP model to identify the damages in a composite cantilevered beam, in which the damage was modeled as delamination in the FEM model of beam. Masri et al. (1996) used a MLP model to detect the changes in the dynamic characteristics of a structure-unknown system. Luo and Hanagud (1997) used the NN model with the dynamic learning rate steepest descent (DSD) method to carry out the real-time flaw detection of composite materials. Zhao et al. (1998) used a counter-propagation NN model to identify the damages in

beams and frames. Liu et al. (1999) used the BRANN model to detect the impact damages in carbon fiber reinforced polymer composite laminates, the transient acoustic emission waveforms detected from the surface of materials were used as the input of BRANN model. The more application of the NN model in the area of damage detection can be found in Bishop (1994) and Doebling et al. (1996).

In this study, a new technique using the adaptive MLP model for the detection of cracks in anisotropic laminated plates is proposed. The displacement response on the surface of plates, excited by a time-harmonic input load, is used as the input of the adaptive MLP model. The crack parameters that specify the location and size of cracks are taken as the output of MLP. Similar to what were described by Chang et al. (2000), this MLP model is first trained using the elaborated sample data of various types of the crack possibilities and their resulting displacement responses on the surface of plate that are calculated using the SEM model. To facilitate this training process, the correlation analysis for the outputs of neurons in the hidden layers of MLP model is carried out to optimize the MLP architecture. A modified back-propagation (BP) learning algorithm with a dynamically adjusted learning rate and an additional jump factor is developed to alleviate the oscillation and stagnation in the training process so as to speed up the convergence of the MLP model. The concept of orthogonal array (OA) is adopted to generate the representative combinations of the crack parameters for significantly reducing the number of samples while maintaining its data completeness. This trained MLP model is then used to reconstruct the crack location and size parameters in the anisotropic laminated plate by feeding in the measured surface displacement response. These reconstructed crack parameters are taken into the SEM model to calculate the displacement response on the plate surface, so as to examine whether or not these calculated response matches satisfactorily the measured ones. If not, the MLP model would go through another round of retraining process until the satisfactory match is reached. To verify the proposed technique numerically, an anisotropic laminated plate $[C0/G+45/G–45]_s$ with horizontal crack was investigated for four different crack situations. The effect of noise involved in the displacement response on the detection results was also examined. Numerical results show that the proposed technique is very effective for the detection of cracks in anisotropic laminated plates.

2. Problem studied and solving strategy

2.1. Problem studied

Fig. 1 shows a composite laminated plate that consists of M anisotropic layers. The thickness of the plate in z direction is denoted by H, both the length and depth of the plate in x and y direction, respectively, are considered to be infinite. This problem is hence two-dimensional. A horizontal crack was assumed to hide inside this plate, whereby its location is defined by the distance a_c (from the plane $x=0$ to the left tip of crack in x direction) and the depth d_c (from the upper surface of the plate to the center of crack in z direction). The size of crack is denoted by l_c.

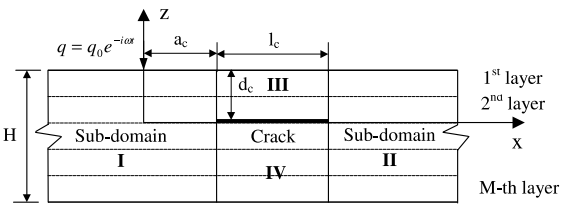

Fig. 1. A M-layers anisotropic laminated plate with a horizontal crack.

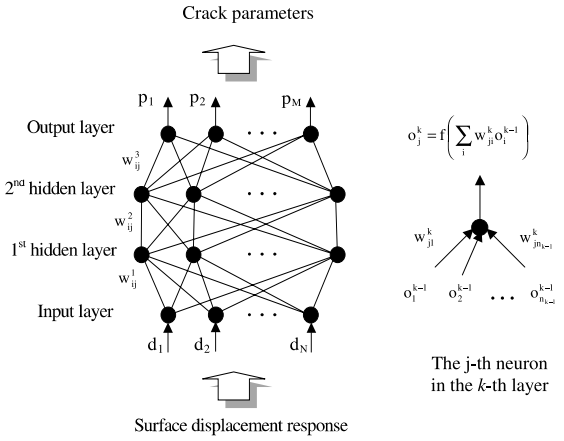

Fig. 2. A MLP model with two hidden layers.

The material of each layer in this plate is anisotropic and inhomogeneous. The elastic constants, the fiber orientation and the density of the mth $(m = 1, \ldots, M)$ layer are denoted by c_{mij} $(i, j = 1, 6)$, ϕ_m and ρ_m, respectively.

A time-harmonic input load q_0, which does not vary in the y direction, was applied on the upper surface of the plate. This load was expressed as

$$q_0 = \overline{q}_0 e^{-i\omega t} \tag{1}$$

where $\overline{q}_0$ and ω are the load amplitude and frequency, respectively. The excited displacement response on the surface of this plate consists of a number of waves scattered due to the crack. It is used as the known information for the crack detection.

The objective of this study is to examine the feasibility of using the adaptive MLP model (as shown in Fig. 2) to detect the location and size of crack hidden in this plate. The excited surface displacement response is used as the input of the MLP model.

2.2. Solving strategy

The proposed solving strategy for the studied problem is shown in Fig. 3. It includes (i) initial training of the MLP model using the elaborated sample data, (ii) reconstruction of the crack parameters using the trained MLP model by feeding in the measured displacement response on the surface of plate. If the reconstructed crack parameters result in the displacement response that significantly differs from the measured ones, the MLP model should be re-trained in order to obtain an improved set of crack parameters.

The purpose of initial training is to establish a preliminary nonlinear mapping relationship between the excited displacement response amplitudes on the surface of plate, $D = \{d_i, i = 1, \ldots, n\}$, and the crack parameters, $P = \{a_c, d_c, l_c\}$. The training samples consist of sets of assumed P_i $(i = 1, \ldots, p)$, representing p types of crack possibilities and the resulting scattered displacement responses that are calculated using the SEM model. Details on the selection of training samples will be discussed in Section 4.3.

After the initial training of the MLP model, reconstruction of the crack parameters begins by feeding the measured response amplitudes D_m into the MLP model. The output of the MLP model would be the reconstructed crack parameters P_r. These reconstructed parameters are then taken into the SEM model to

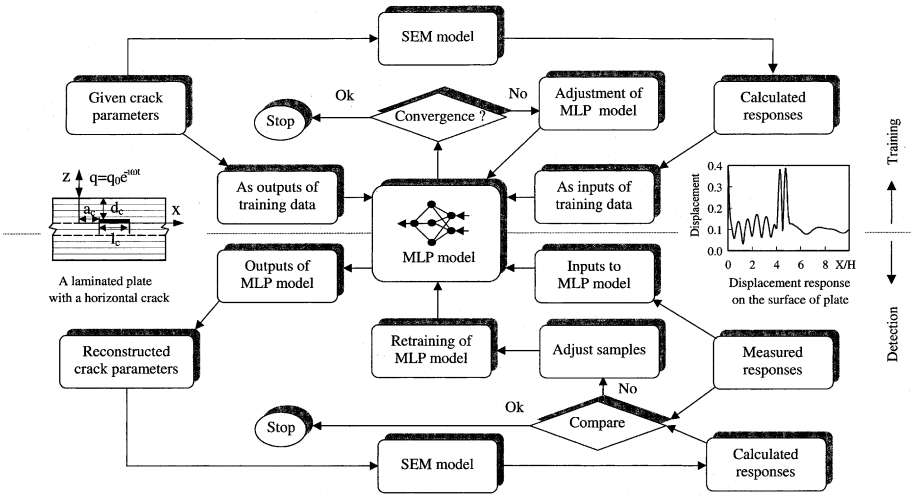

Fig. 3. Proposed strategy for training and application of the MLP model.

calculate the corresponding response amplitudes D_c. A comparison between the calculated responses D_c and the measured ones D_m is made based on the following Euclidean criterion,

$$Eu = \|D_c - D_m\|_2 \tag{2}$$

If Eu is larger than the permissible error Ec, then the MLP model should be retrained on-line using the adjusted sample data that contain D_c and P_r. The retrained MLP model is then used to reconstruct the crack parameters again by feeding in the measured D_m. This procedure would be repeatedly conducted until $Eu \leqslant Ec$, which means that the crack parameters finally reconstructed would be able to produce the surface displacement response that is sufficiently close to the measured ones.

The proposed strategy is conceptually straightforward. There are however two key factors governing the success of this technique in the practical applications. One is that there must be an effective numerical method for calculating the elastic waves scattered due to the cracks in the composite laminated plate, so as to provide the necessary training samples. This requirement is especially true for the cases where the sample data are expensive or difficult to obtain experimentally. Only if these sample data are accurately obtained, the MLP model trained by these data could truthfully simulate the real relationship between the crack parameters and the resulting displacement response on the plate surface. Another governing factor would be that the MLP model shall have the proper network architecture, the good learning algorithm and also trained by the proper sample set, so as to ensure the MLP model to have speedy and accurate convergence. It also ensures the completeness of the trained MLP model for various types of applications. These two issues will be addressed in more detail below.

3. Calculation for scattered displacement response using strip element method

As stated above, effective calculation for the displacement response scattered by the cracks is one of keys to implement the proposed detection technique. As SEM has been verified to be particularly effective for analyzing the scattering of the elastic waves in the composite laminated layers (Liu and Achenbach, 1995), it was thus adopted in this study for the calculation of the scattered displacement responses.

For the anisotropic laminated plate with a horizontal crack shown in Fig. 1, it was divided into four sub-domains denoted by I, II, III and IV, respectively. In each sub-domain, n_i (i = I, II, III and VI) strip elements were further divided along its thickness. In each strip element, saying the strip element k, the governing differential equation (in the case free of body force) can be drawn as follows by following the Kausel's formulation:

$$\rho_k \frac{\partial^2 U_k}{\partial t^2} = D_{kxx} \frac{\partial^2 U_k}{\partial x^2} + 2D_{kxy} \frac{\partial^2 U_k}{\partial x \partial y} + D_{kyy} \frac{\partial^2 U_k}{\partial y^2} \tag{3}$$

where the coefficient matrices D_{kxx}, D_{kxy} and D_{kyy} are given in Appendix A, and the displacements U_k

$$U_k(x,z) = \{\, u_k(x,z) \quad w_k(x,z) \,\}^{\mathrm{T}} \tag{4}$$

According to SEM's theory, it is expressed as:

$$U_k(x,z) = N_k(z) V_k(x) \mathrm{e}^{-\mathrm{i}\omega t} \tag{5}$$

where t and ω are the time and angular frequency, respectively. $\mathrm{i} = \sqrt{-1}$. Interpolation function matrix $N_k(z)$ and displacement amplitude matrix $V_k(x)$ are given below

$$N_k(z) = \left[\left(1 - 3\tfrac{z}{h} + 2\tfrac{z^2}{h^2}\right) I \quad 4\left(\tfrac{z}{h} - \tfrac{z^2}{h^2}\right) I \quad \left(-\tfrac{z}{h} + 2\tfrac{z^2}{h^2}\right) I \right] \tag{6}$$

$$V_k(x) = \left\{\, V_{k\mathrm{l}}^{\mathrm{T}} \quad V_{k\mathrm{m}}^{\mathrm{T}} \quad V_{k\mathrm{u}}^{\mathrm{T}} \,\right\}^{\mathrm{T}} \tag{7}$$

where I is a 2×2 identify matrix and h is the thickness of the strip element k. $V_{k\mathrm{l}}$, $V_{k\mathrm{m}}$ and $V_{k\mathrm{u}}$ are the displacement amplitude vectors on the lower, middle and upper node lines, respectively.

Applying the principle of virtual work to the studied strip element k, we have

$$\delta V_k^{\mathrm{T}} q_k = \delta V_k^{\mathrm{T}} S_k + \int_0^h \delta U_k^{\mathrm{T}} W_k \,\mathrm{d}x \tag{8}$$

where q_k is the external traction vector acting on the three node lines of the element k. S_k is the stress vector on the boundary lines of the element k. By integrating over the thickness of the element, and requiring that the result is valid for arbitrary virtual displacements δV_k, the following differential equation for the studied element k is obtained:

$$\overline{q}_k = -A_{k2} \frac{\partial^2 V_k}{\partial y^2} + A_{k1} \frac{\partial V_k}{\partial y} + A_{k0} V_k - \omega^2 M_k V_k \tag{9}$$

where $\overline{q}_k$ is the amplitude vector of q_k. Matrices A_{k2}, A_{k1}, A_{k0} and M_k are given in Appendix A.

Assembling Eq. (9) for all the strip elements in one sub-domain as what is done in FEM, and analytically solving the integrated equation using the method proposed by Liu and Achenbach (1994) with the consideration of the boundary conditions in the studied sub-domain i, an algebraic equation can be drawn as follows:

$$R_{vi} = K_i V_{vi} + S_{vi} \tag{10}$$

where R_{vi}, V_{vi} and S_{vi} are the external traction vector, displacement vector and the equivalent external force vector, respectively. All these vectors act only on the vertical boundaries of the studied sub-domain i. K_{vi} is the stiffness matrix for this sub-domain.

For each sub-domain i (i = I, II, III and IV), the equation similar to Eq. (10) can be obtained using the same method. Then, integrating these equations for all the sub-domains using the displacement continuity and force equilibrium conditions at the junctions of sub-domains, a set of integrated equations for the cracked laminate are obtained as follows,

$$R = KV + S \tag{11}$$

where R, V and S are the external tractions, displacements and the equivalent external forces acting on all the junctions, respectively. For the given R and the forces on the free surfaces of crack, the displacements V can be obtained by solving the above equations. Finally, the whole displacement field in the studied plate can be obtained. As expected, the displacement field is affected by the location and size of crack hidden in this plate.

4. Adaptive multiplayer perception model

Fig. 2 shows a typical MLP Model. It consists of input, output layer and two hidden layers. Each layer contains some neurons with a nonlinear activation function. In theory, this MLP model can be used to model arbitrary complex nonlinear relationship between the input and output of the studied system. However, the successful application of MLP in practical engineering depends greatly on the topologic architecture, the learning algorithm and the training samples chosen for the MLP model.

4.1. Multiplayer perception architecture

Generally, the number of neurons in the input and output layers for the MLP model is directly determined by the studied problem. In this study, they are the number of surface nodes at which the displacement response is acquired and the number of crack parameters to be reconstructed, respectively.

Two hidden layers have been usually recommended for most of the structural problems (Masri et al., 1996), although one hidden layer was theoretically demonstrated to be sufficient to model arbitrary complex nonlinear relationship (Chen and Chen, 1996). So the most difficult task related to the MLP architecture is to determine the number of neurons in each hidden layer, which is usually completed by using numerical experiments (trial and error). It is often tedious.

One effective method is proposed in this study to tackle this problem. The basic idea is given as follows: For a hidden layer being adjusted, a larger neuron number is selected at first, the correlativity γ_{ij} between the output of the ith neuron and the output of the jth neuron, and a criterion parameter α_i are then calculated as follows.

$$\gamma_{ij} = \frac{\overline{o}_{ij}}{\sqrt{\overline{o}_i \overline{o}_j}}, \qquad \alpha_i = \sum_{j=1}^{m} \gamma_{ij}, \quad i, j = 1, \ldots, m \tag{12}$$

where

$$\overline{o}_i = \sum_{k=1}^{p} o_{ik}^2 - \frac{\sum_{k=1}^{p} o_{ik}}{p}, \qquad \overline{o}_j = \sum_{k=1}^{p} o_{jk}^2 - \frac{\sum_{k=1}^{p} o_{jk}}{p}, \qquad \overline{o}_{ij} = \sum_{k=1}^{p} o_i o_j - \frac{\sum_{k=1}^{p} o_{ik} \sum_{k=1}^{p} o_{jk}}{p} \tag{13}$$

m is the current number of neurons, p is the number of the total training samples, o_{ik} is the output of the ith neuron for the kth sample.

If $\gamma_{\max} = \max(\gamma_{ij}) \geqslant \gamma_c$ (in general, $\gamma_c = 0.8$–0.9) in this hidden layer, those neurons with larger α_i value would be first cancelled out. Then, $\gamma_{\max}$ and α_i are calculated again with the adjusted number of neurons. This process is continually repeated until $\gamma_{\max} < \gamma_c$ in this hidden layer. It is obvious that the over abundance of neurons in one hidden layer can be eliminated by this way. The proper MLP architecture is then obtained.

4.2. Learning algorithm

Most of the training for the MLP model is based on the back propagation (BP) learning algorithm, this algorithm usually results in oscillation or stagnation in the training process. In this study, a modified BP learning algorithm with a dynamically adjusted learning rate and a jump factor is adopted to solve this problem and thus speed up the convergence of the MLP model.

Mathematically, the output of the MLP model can be expressed as follows:

$$P = g(W, \theta, D) \tag{14}$$

where

$$W = \{w_{ij}^k\} \quad i = 1, \ldots, m_i, \ \ j = 1, \ldots, m_j, \ \ k = 1, 2, 3$$

$$\theta = \{\theta_j^k\} \quad j = 1, \ldots, m_j, \ \ k = 1, 2, 3$$

w_{ij}^k and θ_j^k are the weight and bias term of networks, m_i and m_j are the number of neurons in the ith and the jth layer, respectively. D is the input of the MLP model.

Training of the MLP model is actually referred to a process of determining the weight matrix W and the bias matrix θ, so as to make the output $P = \{p_i, i = 1, \ldots, m_3\}$ equal to its targeted value $P_t = \{p_{ti}, \ i = 1, \ldots, m_3\}$. That means the error norm $E(W, \theta)$

$$E(W, \theta) = \frac{1}{2} \sum_{i=1}^{p} \left(1 - \frac{p_i}{p_{ti}}\right)^2 \tag{15}$$

becomes smaller than a tolerable value.

As the bias term can be treated as a special weight in the training of the MLP model, the adjustment for both W and θ can be written as:

$$W^{r+1} = W^r + \Delta W^r \tag{16}$$

$$\Delta W^r = -\eta \frac{\partial E(W, \theta)}{\partial W}\bigg|_{W=W^r} + \alpha\eta \frac{\partial E(W, \theta)}{\partial W}\bigg|_{W=W^{r-1}} \tag{17}$$

where η is defined as the learning rate, α is the momentum rate, and r is the number of iterations in training. The derivatives in Eq. (17) are matrices whose arguments can be found as,

$$\frac{\partial E(W, \theta)}{\partial w_{ji}^k} = \frac{\partial E(W, \theta)}{\partial \mathrm{net}_j^k} \frac{\partial \mathrm{net}_j^k}{\partial w_{ji}^k} = -\delta_j^k \cdot o_i^{k-1} \tag{18}$$

Note that net_j^k and o_i^k represent the input and the output of the ith neuron in the kth layer, respectively.

$$\mathrm{net}_j^k = \sum_i w_{ji}^k o_i^{k-1}, \qquad o_j^k = f(\mathrm{net}_j^k), \qquad f(\mathrm{net}_j^k) = \frac{1}{1 + \mathrm{e}^{-(\mathrm{net}_j^k + \theta_j)}} \tag{19}$$

δ_j^k can be expressed as,

$$\delta_j^k = \frac{1}{p_{tj}} \left(1 - \frac{p_j}{p_{tj}}\right) f'(\mathrm{net}_j^k) \quad \text{in output layer, } \ k = 3 \tag{20a}$$

or

$$\delta_j^k = \left(\sum_i \delta_i^{k+1} \mathrm{w}_{ij}^{k+1}\right) f'(\mathrm{net}_j^k) \quad \text{in hidden layers, } \ k = 1, 2 \tag{20b}$$

and $f'(\mathrm{net}_j^k)$ is the first derivative of the activation function $f(\cdot)$ with respect to net_j^k. The activation function used in this study is a sigmoid function as shown in Eq. (19).

Vogl et al. (1988) and Luo and Hanagud (1997) proposed the improved methods to accelerate the convergence of the MLP model by dynamically varying the learning rate η in training. The similar idea is also employed in this study. The learning rate η is adjusted once every k_n iterations instead of every iteration as usually done for increasing the stability of the modified algorithm. Assuming that the learning rate for the nth iteration is represented by $\eta(n)$, this learning rate will be adjusted at the $(n+k_n)$th iteration based on the following criterion:

$$\eta(n+k_n) = c\eta(n) \tag{21}$$

where the range of c is selected in the following manner based on the numerical experiments,

$$\begin{aligned} c &= 1.1\text{–}1.3 \quad \text{if } \ 0 < e_n(i) < \varepsilon_1, \ \ i = 1,2,\ldots,k_n \\ &= 0.7\text{–}0.9 \quad \text{if (number of negative } e_n(i), \ \ i = 1,2,\ldots,k_n) \geqslant \varepsilon_2 \\ &= 1.0 \quad \text{if else} \end{aligned} \tag{22}$$

The error rate $e_n(i)$ is defined as,

$$e_n(i) = \frac{E(W^{n+i},\theta^{n+i}) - E(W^{n+i+1},\theta^{n+i+1})}{E(W^{n+i},\theta^{n+i})} \quad i = 1,2,\ldots,k_n \tag{23}$$

Numerical studies suggest that k_n is selected between 10 and 50, ε_1 between 0.001 and 0.01, and ε_2 between $0.1k_n$ and $0.5k_n$, respectively.

The change of weights, Δw_{ij}^k, which is directly related to the training of the MLP model, is not only dependent on the learning rate η, but also on the partial derivative $\partial E(W,\theta)/\partial w_{ji}^k$ (see Eqs. (17)–(20)). Riedmiller and Braun (1993) pointed out the possibility that the effect of the carefully adapted η can be drastically disturbed by the unforeseeable behavior of the derivative itself. In fact, this problem mainly comes from the possible saturation of sigmoid function, i.e., $f'(\mathrm{net}_j^k) \to 0$, which leads to $\delta_j^k \to 0$ and causes the weight matrix to stagnate. To solve this potential problem, a jump factor γ is added to $f'(\mathrm{net}_j^k)$ in Eq. (20), so as to always maintain a non-zero value of δ_j^k, and thus prevents the weight matrix from stagnation.

$$\delta_j^k = \frac{1}{p_{\mathrm{t}j}}\left(1 - \frac{p_j}{p_{\mathrm{t}j}}\right)\left\{f'\left(\mathrm{net}_j^k\right) + \gamma\right\} \quad \text{in output layer, } \ k = 3 \tag{24a}$$

or

$$\delta_j^k = \left(\sum_i \delta_i^{k+1} \cdot w_{ij}^{k+1}\right)\left\{f'\left(\mathrm{net}_j^k\right) + \gamma\right\} \quad \text{in hidden layers, } \ k = 1,2 \tag{24b}$$

γ varies during the training process. It is recommended to select between 0 and 0.5.

4.3. Training samples

Rogers (1994) indicated that in addition to the proper networks architecture and the efficient learning algorithm, the selection of training samples is another key factor in obtaining a reliable MLP model for the studied problem. Generally, an ideal set of training samples should be complete, i.e. be able to represent the total sample space. That means the combinations of crack parameters in training samples should be able to cover all the crack possibilities for this study.

One common method to this end is to use complete combination method (Manson et al., 1989). For the cases where there are p crack parameters, and each parameter comes with q discrete values, the number of all the possible combinations is q^p. Although the completeness of samples is guaranteed by

these q^p samples, the number is however prohibitively large and obviously impractical to include all the samples for the complex engineering problems. Another simplified method with the similar idea is to use a hypercube to cover the samples space (Manson et al., 1989), but the number of the required samples is still larger. The linear method (Rogers, 1994) generates the training samples by starting at the lower bound of each parameters and then stepping through the sample space at a given increment until reaching the upper bound. It seems to be too simple for representing the sample space. Recently, Atalla and Inmam (1998) suggested that the random generation of the characteristic parameters (i.e. the crack parameters in this study) within their variation ranges could produce a good training result. Levin and Lieven (1998) proposed a two-part scheme. The first part consisted of assigning each parameter in turn to one of the q discrete values while giving all the other parameters to their respective nominal values. The second part consisted of generating a given number of training samples by adjusting a random selection of the p values by a random amount.

In this study, we adopt the OA method to generate the representative training samples. The OA was originally developed for the experimentalists to reduce the number of experimental trials normally required in a full factorial experimental design (Manson et al., 1989). With this OA method, only $p(q-1)+1$ rather than q^p combinations are required for representing the total sample space for the same case stated above, if there is no interaction among the p parameters. The number $p(q-1)+1$, which is determined by the corresponding OA $L_A(q^p)$ where $A = p(q-1)+1$ (Besterfield et al., 1995), is significantly smaller than the complete sample number of q^p, especially when the number of parameters and/or their discrete values to be considered are large. It is however able to guarantee the completeness of samples. In addition, as each sample is orthogonal to the others among these $p(q-1)+1$ samples, the effect of each parameter on the trained MLP model will tend to be accurate and reproducible.

A concrete configuration for the $p(q-1)+1$ samples, i.e. a properly selected value of each parameter in each sample, is implemented in the same strategy as what is done in quality engineering (Besterfield et al., 1995).

Another difficulty related to the training samples is how to adjust the current sample data during the retraining process of the MLP model. It is not straight forward to improve the accuracy of output of the retrained MLP model by only further reduction of the permissible error norm. A reasonable solution would be to continuously replace some unnecessary sample data by those newly generated ones that are expected to be more close to the real solution of problem under investigation with the retraining process. These new sample data are obtained from the output of the MLP model in the preceding retraining round and their resulting displacement responses calculated from the SEM model. These replaced samples, (D_i, P_i), are the ones that have the largest Euclidean distance l_i from the measured displacement responses D_{m}.

$$l_i = \|D_{\mathrm{m}} - D_i\|_2 \tag{25}$$

It is obvious that the sample density around the real solution of problem increases as the retraining process takes place. As a result, the modeling accuracy of the MLP model in the neighborhood of the real solution would be improved.

Finally, the sample data are required to normalize based on the following formulation before used in the training of the MLP model,

$$\bar{x}_i = \frac{x_i - \beta x_{i_{\min}}}{\alpha x_{i_{\max}} - \beta x_{i_{\min}}} \tag{26}$$

where $x_{i\max}$ and $x_{i\min}$ are the maximal and minimal values of parameter x in the sample data, respectively; $\bar{x}_i$ is the normalized value of parameter x ranging between 0 and 1. The coefficients are: $\alpha = 1.1$, $\beta = 0.9$ (if $x_{i\min} \geqslant 0$) or 1.1 (if $x_{i\min} < 0$). This normalization ensures that the samples data would not be too close to 0 or 1 so as to avoid numerical difficulties during the training process.

5. Numerical examples

The above proposed detection technique was examined using an anisotropic laminated plate denoted by $[C90/G+45/G–45]_s$, where C and G stand for carbon/epoxy and glass/epoxy layers, respectively. The number following the alphabet denotes the fiber orientation with respect to the x-axis, and the subscript s denotes that the plate is symmetrically stacked. Material constants of carbon/epoxy and glass/epoxy are given in Table 1.

Each layer in this plate was divided into four strips in thickness direction. The number of the total strips is hence 24. The horizontal crack was assumed to locate at the junctions of two adjacent strip elements. The time harmonic line load q_0 with amplitude $\overline{q}_0 = 1$ and frequency $\omega = 3.14\sqrt{c_{44}/\rho}/H$ was applied on the upper surface of plate at $x = 0$. The surface displacement response was measured and used to detect the crack in the plate.

For the sake of simplicity, the following dimensionless parameters were used in this study:

$$\overline{x} = \frac{x}{H}, \quad \overline{w} = \frac{c_{44}w}{q_0}, \quad \overline{\omega} = \frac{\omega H}{\sqrt{c_{44}/\rho}}, \quad \overline{a}_c = \frac{a_c}{H}, \quad \overline{d}_c = \frac{d_c}{H}, \quad \overline{l}_c = \frac{l_c}{H} \tag{27}$$

Figs. 4–6 give the displacement response amplitudes in the vertical direction on the upper surface of plate under different crack situations. By comparing Figs. 4 and 5, it can be observed that there is a ''special region'', which results from the waves scattered due to the crack. It reveals the significant change in both amplitude and pattern of the response within this region. This ''special region'' shifts horizontally in the same direction as the crack moves. The effect of the crack location a_c on the displacement response is thus obviously exhibited. By comparing the Figs. 4 and 6, it can be observed that the maximal amplitude of the response within the ''special region'' decreases with the increase of the crack depth d_c. From each of these three figures, the effect of the crack size l_c on the displacement response can be observed. With the decrease of l_c, the amplitudes of the oscillated displacement response within the ''special region'' obviously mitigate. When $l_c = 0$, i.e. noncrack case, the ''special region'' disappears. These observations demonstrate that the information on the crack is indeed encoded by the surface response of the plate. This provides us with possibility of using the surface response as the input of the MLP model to detect the cracks in the plate.

In order to detect the possible shortest crack in horizontal direction and simultaneously avoid the over complexity of the MLP architecture, the response amplitude at 34 selected nodes on the surface of plate within the region from $\overline{x} = 0$ to $\overline{x} = 10$ were used as the input of the MLP model. Consequently, the number of neurons in the input layer of MLP is 34, and the minimal length $\overline{x}_{min}$ for the detectable crack is therefore about $10H/(34-1) = 0.3H$. The crack parameters $\overline{a}_c$, $\overline{d}_c$ and $\overline{l}_c$ were used as the output of the MLP model, so the number of neurons in the output layer of MLP is 3. Two hidden layers were employed in this study as usually done (Chang et al., 2000). The number of neurons for the first and second hidden layers was initially assigned to be 45 and 20, respectively.

To formulate the initial training samples, it was assumed that there were six levels of discrete values for these three crack parameters $\overline{a}_c$, $\overline{d}_c$ and $\overline{l}_c$ (Table 2).

Table 1
Material constants of the laminated plate

	E_1 (GPa)	E_2 (GPa)	G_{12} (GPa)	ν_{12}	ν_{23}	ρ (g/cm^3)
Carbon/epoxy	142.17	9.255	4.795	0.3340	0.4862	1.90
Glass/epoxy	38.49	9.367	3.414	0.2912	0.5071	2.66

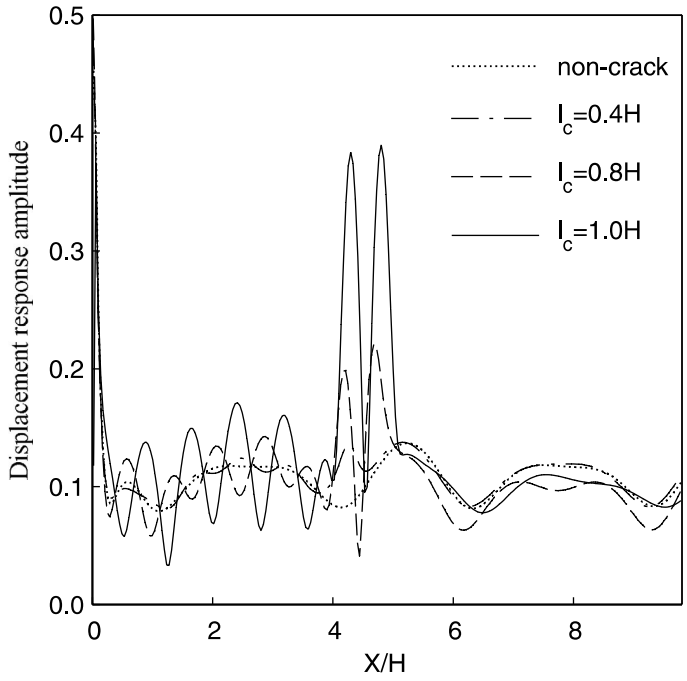

Fig. 4. Amplitudes of the displacement responses on the surface of plate ($a_c = 4H,\ d_c = 4H/24$).

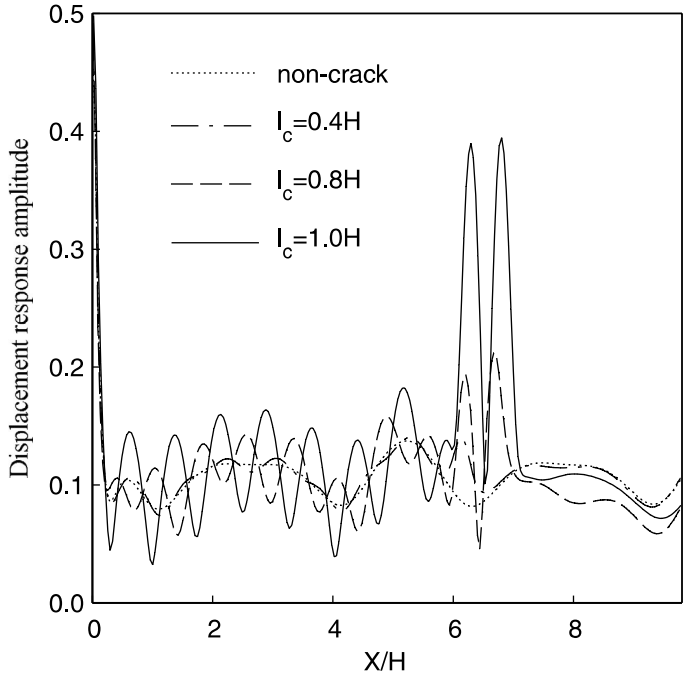

Fig. 5. Amplitudes of the displacement responses on the surface of plate ($a_c = 6H,\ d_c = 4H/24$).

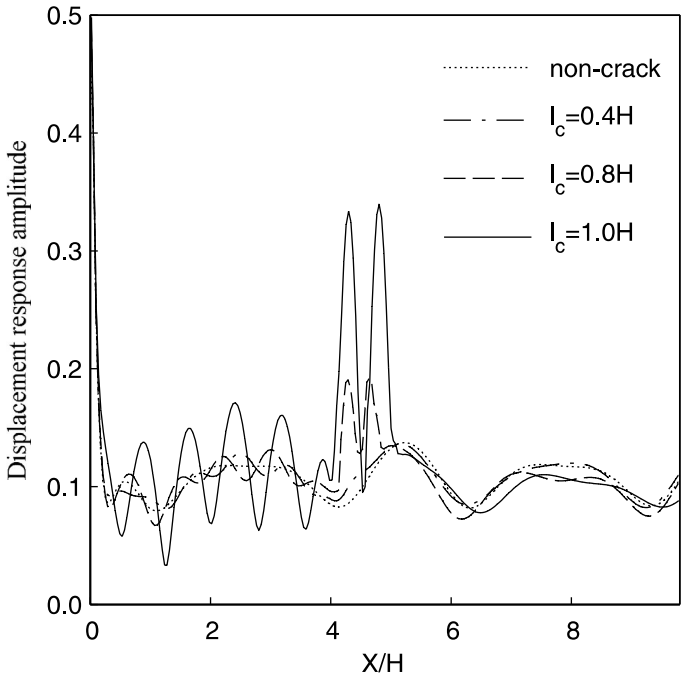

Fig. 6. Amplitudes of the displacement responses on the surface of plate ($a_c = 4H,\ d_c = 8H/24$).

Table 2
The discrete values of crack parameters

	Level 1	Level 2	Level 3	Level 4	Level 5	Level 6
$\bar{a}_c$	0	1	3	5	6	8
$\bar{d}_c$	2/24	4/24	8/24	12/24	16/24	20/24
$\bar{l}_c$	0.3	0.6	0.9	1.2	1.5	1.8

It would need a total of $6^3 = 218$ combinations to cover all the crack possibilities by applying the complete combination method for this case. However, based on the OA method proposed in section 4.3 and employing the corresponding OA $L_{16}(6^3)$, only $3 \times (6-1)+1 = 16$ combinations were required to cover the whole sample space. To further reinforce the sample set, it was decided to add six samples that come from varying each crack parameter to its extreme value in turn while keeping other two crack parameters at their reference values.

The SEM was used to calculate the displacement response on the surface of plate for each of these 22 combinations so as to generate 22 initial samples. These samples were then normalized by Eq. (26) and used for the training of the initially designed MLP model above. The modified BP learning algorithm with the initial $\eta = 2.0$, $\alpha = 0.5$, $\gamma = 0.05$ outlined in Section 4.2 was used in this training. The number of neurons in two hidden layers was also adjusted according to the criterion described in Section 4.1. Finally, the number of 24 and 9 was obtained for first and second hidden layers, respectively. For this optimized MLP architecture, the given convergence criterion was fulfilled after 7032 training iterations. The convergence of the error norm $E(W,\theta)$ within the first 5000 iterations is shown in Fig. 7.

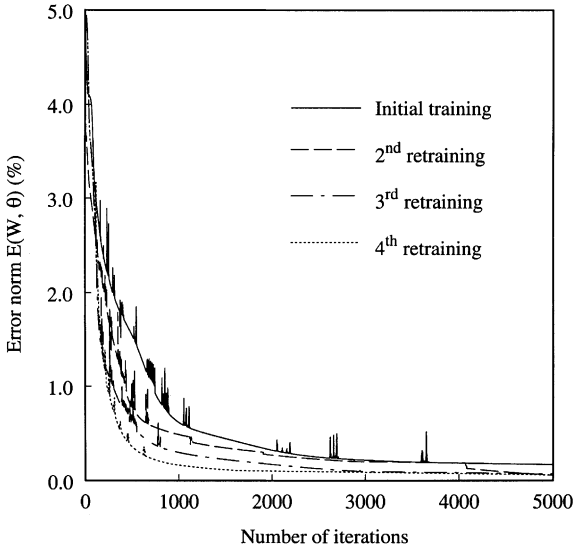

Fig. 7. Convergence of the MLP model in training process.

5.1. Response data without noise

To validate the proposed technique, four simulated crack cases were introduced in this plate: (1) $\overline{a}_c = 4.5$, $\overline{d}_c = 4/24$, $\overline{l}_c = 0.5$; (2) $\overline{a}_c = 7$, $\overline{d}_c = 4/24$, $\overline{l}_c = 1$; (3) $\overline{a}_c = 4.5$, $\overline{d}_c = 8/24$, $\overline{l}_c = 0.5$; and (4) $\overline{a}_c = 7$, $\overline{d}_c = 8/24$, $\overline{l}_c = 1.0$. All these cases have not been involved in the training samples for examining the detecting capability of the trained MLP model. The resulting displacement responses on the surface of plate calculated from the SEM model with these cracks were simulated as the measured responses (Fig. 8). These

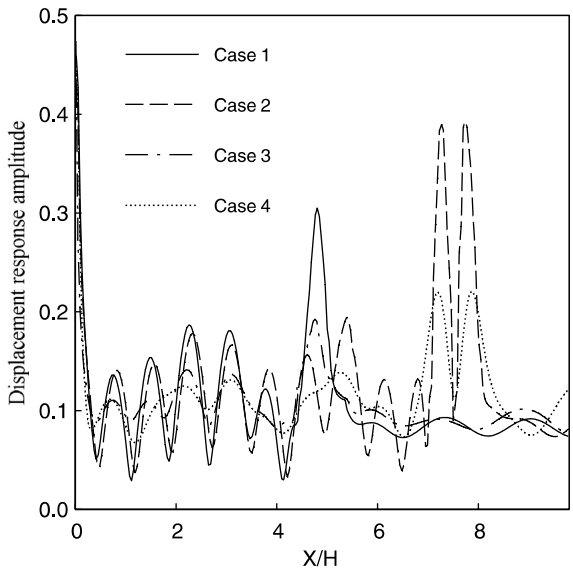

Fig. 8. Displacement response amplitudes on the surface of plate which are used as the input of the MLP model.

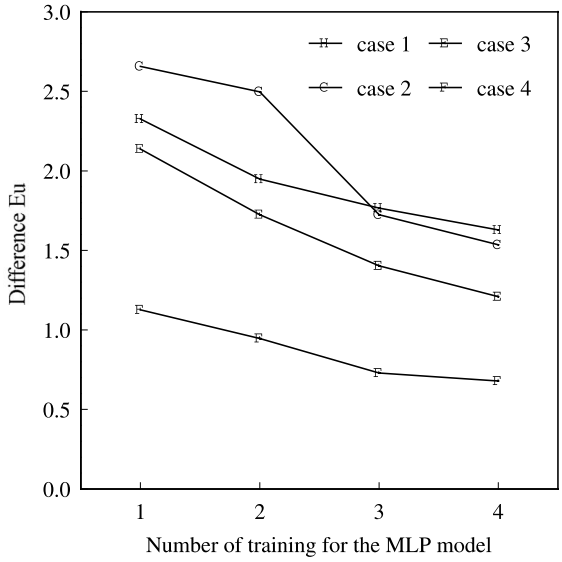

Fig. 9. Changes of the difference *Eu* between the calculated and the simulated displacement response amplitudes.

simulated responses were used as the inputs of the trained MLP model to reconstruct these crack parameters.

The first reconstructions of crack parameters were immediately obtained by feeding the simulated responses into the trained MLP model for four crack cases. In order to examine the accuracy of the output from the MLP model, these reconstructed crack parameters were then put into the SEM model to calculate the surface displacement responses of the plate. It can be found from Fig. 9 that these calculated responses are significantly different from the simulated ones in terms of *Eu* for all the four cases. In fact, the maximal error for the reconstructed $\overline{a}_c$, $\overline{d}_c$ and $\overline{l}_c$ was as high as -23.44%, -22.34%, -24.94% and -22.98% for the four cases, respectively. Obviously, the reconstructions were not acceptable. The retraining procedure for the MLP model outlined in Section 2.2 was thus required. Four new samples were consequently generated from these reconstructed crack parameters and the resulting displacement responses calculated from the SEM model. These new samples were then put into the original sample set while four selected samples were simultaneously canceled out. The MLP model was retrained with the adjusted sample set, and then used to reconstruct the crack parameters again. With the progress of this retraining process, the displacement responses calculated from the SEM model with the reconstructed crack parameters became more and more close to the simulated ones. As one of examples, Fig. 10 shows the evolution process of the calculated displacement response amplitudes for case (2). After three times of retraining, the displacement responses calculated from the reconstructed crack parameters were likely very close to the simulated ones for all the four cases. Further retraining for the MLP model did not seem to significantly decrease the Euclidean criterion *Eu*, which quantitatively depicts the difference between the calculated and the simulated displacement response. The maximum error of the reconstructed crack parameters with respect to their assumed values decreases to -5.03%, -4.92%, -6.84% and -5.43%, respectively. Fig. 11 shows the convergence of these crack parameters during the reconstruction process. The convergence of the error norm $E(W,\theta)$ for the MLP model during the three times of retraining was also shown in Fig. 7. The numerical simulated results demonstrated that the trained MLP model could correctly detect both the location (denoted by $\overline{a}_c$ and $\overline{d}_c$) and the length ($\overline{l}_c$) of crack hidden in the anisotropic laminated plates where no noise is assumed in the response data.

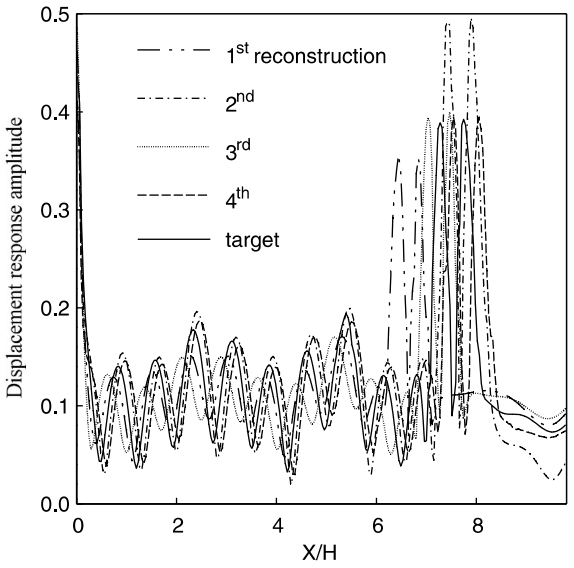

Fig. 10. Evolution process of the calculated displacement response amplitudes.

5.2. Response with noise

To further examine the applicability of the proposed technique for the practical problems where the noise is inevitable in the measured data, the displacement response data acquired from the SEM model were involved with the simulated noise. The noise was generated from a random sample of Gauss distribution with the mean value $a = 0$ and the variance b given by

$$b = p_e \left[\frac{1}{n} \left(\sum_{1}^{n} x_i^2 \right) \right]^{1/2} \tag{28}$$

where p_e is the given noise level, x_i is the displacement response amplitude at node i $(i = 1, \ldots, n)$, n is the node number ($n = 34$ in this study).

For comparing the output from the MLP model using these noisy data as input with that of the non-noise cases, the location and length of cracks assumed in case (1) and case (4) outlined above were reconstructed again. The noise levels of 5% ($p_e = 0.05$) and 10% ($p_e = 0.1$) were given by Eq. (28) and the Guass-random generator for these two cases, respectively. They were then added into the response data simulated from the SEM models. The overall response data with noise were put into the trained MLP model for reconstructing the crack parameters.

Similar to the analysis process outlined in Section 5.1, the first batch of reconstructions from the MLP model for both case (1) and case (4) were not satisfactory. The retaining of the MLP model was then conducted. After four times of successive retraining, the maximal error of crack parameters reconstructed from the MLP model for case (1) converged to -5.03%, -6.14% from -27.61%, -28.42% for the response data with 5% and 10% involved noise, respectively. For case (4), it converged to -6.36%, -6.81% from -27.89%, -29.83% for the same two noise levels, respectively. These reconstructed results are shown in Fig. 12. Based on the results, it is found that the satisfactory reconstruction of the crack parameters is possible from the trained MLP model even if the input is involved with some noise. Of course, more times of retraining for the MLP model would be required.

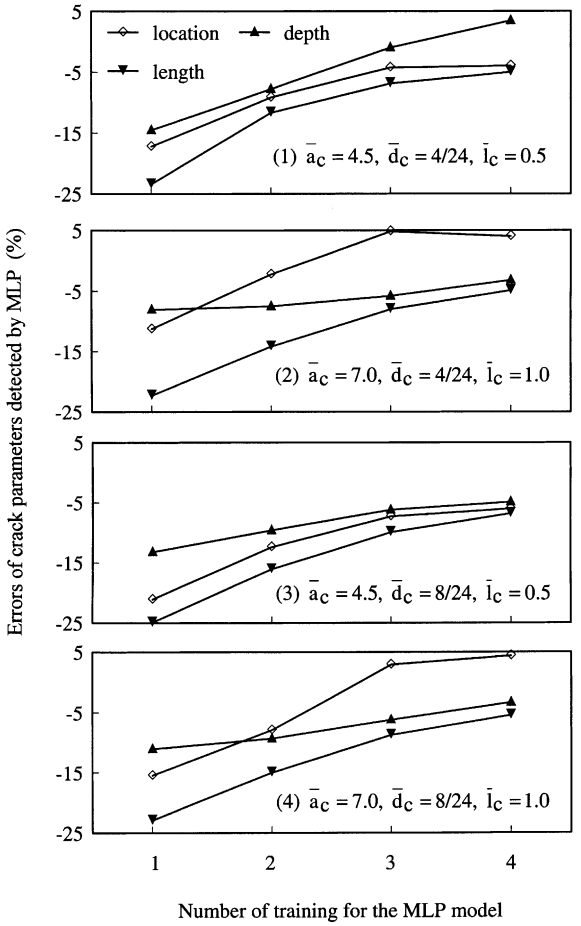

Fig. 11. Errors of crack parameters detected by the trained MLP model without noise in the response data.

5.3. Comments on the numerical results

From Figs. 4–6 and Figs. 11, 12, the following two remarks can be drawn:

(1) Accuracy of the reconstructions from the trained MLP model depends significantly on the sensitivity of the displacement response on the plate surface to the variation of the location and length of cracks. As the longer and shallower the crack is, the more significant the distortion would be in the surface displacement response. Consequently, the better accuracy could be obtained in reconstructing the crack parameters. It is seen in cases (2) and (3), where case (2) has the highest accuracy and case (3) is the lowest among those 4 simulated crack cases.

(2) The proposed MLP technique can withstand the presence of the noise in the response data. This comes from the inherent property of NN techniques, and is known as one of the main advantages of the NN in comparison with the traditional techniques in engineering applications. As the noise inevitably presents in the measured response, robustness in accommodating the noisy response data is usually vital for the successful application of the detection techniques in real engineering.

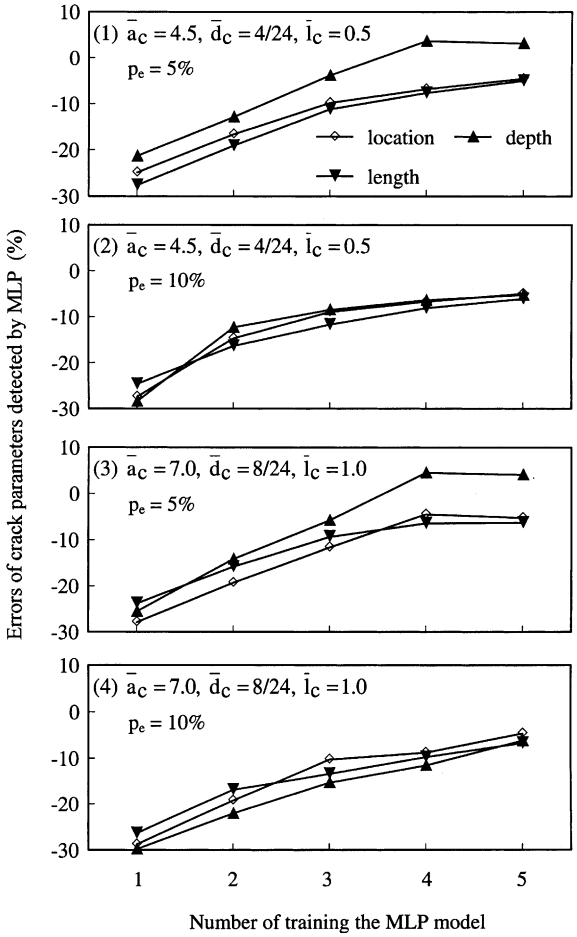

Fig. 12. Errors of crack parameters detected by the trained MLP model with noise in the response data.

6. Conclusions

In this study, an adaptive MLP networks technique for the detection of cracks in anisotropic laminated plates is proposed. The excited displacement response on the surface of plate is used as the input of the adaptive MLP model. The crack parameters, i.e. the location and size of cracks, are used as the output of the MLP model. This MLP model is first trained using the elaborated sample data that contain some types of crack cases and the resulting displacement responses on the plate surface calculated from the SEM model. Several improved numerical methods are proposed to facilitate this training process. The correlation analysis for the outputs of neurons in the hidden layers of MLP is carried out to optimize the number of neurons in each hidden layer. A modified BP learning algorithm with a dynamically adjusted learning rate and an additional jump factor is developed to tackle the possible oscillation and stagnation in training process so as to speed up the convergence of the MLP model. The concept of OA is adopted to generate the representative combinations of crack parameters in order to significantly reduce the number of training samples while maintaining the completeness of sample data. This trained MLP model is then used to re-

construct the crack parameters by feeding in the measured surface displacement response. The reconstructed crack parameters are further examined by checking whether or not the calculated surface displacement response from the SEM model with these reconstructed crack parameters match satisfactorily the measured ones. If not, the MLP model would go through another round of retraining until the satisfactory match is reached.

The proposed technique was verified numerically using an anisotropic laminated plate $[C0/G+45/G–45]_s$ with four types of horizontal cracks located at the different location and with different length. The simulated surface response with and without noise was used as the input of the trained MLP model to detect these cracks. By retraining the MLP model, the reconstructions of crack parameters were gradually improved to the required accuracy for all the simulated cases.

Based on this study, some observations on the detection of cracks in anisotropic laminated plates using MLP technique can be drawn as follows:

(1) The MLP technique is very effective for the detection of cracks in anisotropic laminated plates. One of its advantages is the feasibility for the application in real engineering. Just applying a time-harmonic load on the surface of plate and simultaneously measuring the surface displacement response, the cracks hidden in the plate could be successfully detected. Another attractive feature is its robustness in accommodating the presence of noise in the response data, which is vital to the practical applications.

(2) This detection technique can be effectively implemented with the help of the developed numerical methods. SEM provides an effective approach to calculate the scattered displacement response due to cracks or flaws, the sample data required for the training of the MLP model are thus able to obtain numerically with the satisfactory accuracy. The correlativity analysis method for adjusting the number of neurons in hidden layers of MLP, the OA method for optimizing the sample set, and the modified BP learning algorithm for speeding up the convergence of MLP provide the solid technical support for the implementation of the MLP model in engineering.

(3) From the numerical examinations, it is seen that the accuracy of output from the MLP model improves with the increase of the retraining process. The required accuracy can be reached theoretically by increasing the times of retraining. However, it requires more computational effort. Judgment shall be exercised for a particular crack detection in the real applications.

Acknowledgements

The research is partly supported by the Singapore – MIT alliance program.

Appendix A

Coefficient matrices in Eqs. (3) and (9)

$$D_{kxx}=\begin{bmatrix} c_{k11} & c_{k13} \\ c_{k13} & c_{k33} \end{bmatrix}, \qquad D_{kxy}=\frac{1}{2}\begin{bmatrix} 2c_{k13} & c_{k33}+c_{k12} \\ c_{k33}+c_{k12} & 2c_{k23} \end{bmatrix}, \qquad D_{kyy}=\begin{bmatrix} c_{k33} & c_{k23} \\ c_{k23} & c_{k22} \end{bmatrix}$$

$$A_{k2}=\frac{h}{30}\begin{bmatrix} 4D_{kyy} & 2D_{kyy} & -D_{kyy} \\ & 16D_{kyy} & 2D_{kyy} \\ sy. & & 4D_{kyy} \end{bmatrix}, \qquad A_{ko}=\frac{1}{3h}\begin{bmatrix} 7D_{kxx} & -8D_{kxx} & D_{kxx} \\ & 16D_{kxx} & -8D_{kxx} \\ sy. & & 7D_{kxx} \end{bmatrix},$$

$$A_{k1} = \frac{1}{3h}\begin{bmatrix} 3(D_{kxy} - D'_{kxy}) & -4D_{kxy} & D_{kxy} \\ & 0 & -4D_{kxy} \\ asy. & & -3(D_{kxy} - D'_{kxy}) \end{bmatrix}, \qquad M_k = \frac{\rho_k h}{30}\begin{bmatrix} 4I & 2I & -I \\ & 16I & 2I \\ sy. & & 4I \end{bmatrix},$$

$$D'_{kxy} = \begin{bmatrix} c_{k13} & c_{k12} \\ c_{k33} & c_{k23} \end{bmatrix}$$

References

Atalla, M.J., Inman, D.J., 1998. On model updating using neural networks. Mech. Sys. Signal Proc. 12, 135–161.

Besterfield, D.H., Besterfield-Michna, C., Besterfield, G.H., Besterfield-Sacre, M., 1995. Total Quality Management. Prentice-Hall, New York.

Bishop, C.M., 1994. Neural networks and their applications. Rev. Sci. Instru. 65, 1803–1832.

Chang, C.C., Chang, T.Y.P., Xu, Y.G., 2000. Adaptive neural networks for model updating of structures. Smart Mater. Struct. 9, 59–68.

Chen, T., Chen, H., 1996. Universal approximation capability of EBF neural networks with arbitrary activation functions. Circuits Sys. Signal Proc. 15, 671–683.

Datta, S.K., Ju, T.H., Shah, A.H., 1992. Scattering of an impact wave by a crack in a composite plate. ASME J. App. Mech. 59, 596–603.

Doebling, S.W., Farrar, C.R., Prime, M.B., Shevitz, D.W., 1996. Damage identification and health monitoring of structural and mechanical systems from changes in their vibrations characteristics: A literature review. Tech. Report LA-13070-MS, Los Alamos National Lab., USA.

Karim, M.R., Kundu, T., 1989. Transient response of three layered composites with two interface cracks due to a line load. Acta Mech. 76, 53–72.

Karim, M.R., Kundu, T., Desai, C.S., 1989. Detection of delamination cracks in layered fiber reinforced composite plates. ASME J. Pressure Vessel Tech. 111, 165–171.

Karim, M.R., Kundu, T., 1990. Scattering of acoustic beams by cracked composites. ASCE J. Engng. Mech. 116, 1812–1827.

Karim, M.R., Awal, M.A., Kundu, T., 1992a. Numerical analysis of guided wave scattering by multiple cracks in plates: SH-case. Engng. Fract. Mech. Int. J. 42, 371–380.

Karim, M.R., Awal, M.A., Kundu, T., 1992b. Elastic wave scattering by cracks and inclusions in plates: In-plane case. Int. J. Solids Struct. 29, 2355–2367.

Karunasena, W.M., Shah, A.H., Datta, S.K., 1991. Plane-strain-wave scattering by cracks in laminated composite plates. ASCE J. Engng. Mech. 117, 1738–1754.

Klenke, S.E., Paez, T.L., 1994. Damage identification with probabilistic neural networks. Proc. of the 12 th Int. Modal Anal. Conf. pp. 99–104.

Kundu, T., Hassan, T., 1987. A numerical study of the transient behavior of an interfacial crack in a bimaterial plate. Int. J. Fract 35, 55–69.

Kundu, T., 1988. Dynamic interaction between two interface cracks in a three layered plate. Int. J. Solids Struct. 24, 27–39.

Lam, K.Y., Liu, G.R., Wang, Y.Y., 1997. Time-harmonic response of a vertical crack in plates. Theor Appl. Frac. Mech. 27, 21–28.

Levin, R.I., Leven, N.A.J., 1998. Dynamic finite element model updating using neural networks. J. Sound Vib. 210, 593–607.

Liu, S.W., Datta, S.K., Ju, T.H., 1991. Transient scattering of Rayleigh lamb waves by a surface-breaking crack: Comparison of numerical simulation and experiment. J. Nondestruct. Evaluat. 10, 111–126.

Liu, S.W., Datta, S.K., 1993. Scattering of ultrasonic waves by cracks in a plane. ASME. J. Appl. Mech. 60, 352–357.

Liu, G.R., Achenbach, J.D., 1994. A strip element method for stress analysis of anisotropic linearly elastic solids. Trans. ASME 61, 270–277.

Liu, G.R., Lam, K.Y., 1994. Characterization of a horizontal crack in anisotropic laminated plates. Int. J. Solids Struct. 31, 2965–2977.

Liu, G.R., Achenbach, J.D., 1995. Strip element method to analyze wave scattering by cracks in anisotropic laminated plates. ASME J. Appl. Mech. 62, 607–613.

Liu, G.R., Lam, K.Y., Tani, J., 1995. Strip element method for characterization of flaws in sandwich plates. JSME Int. J. Series A 38, 554–562.

Liu, G.R., Lam, K.Y., Shang, H.M., 1996. Scattering of waves by flaws in anisotropic laminated plates. Composites: part B. 27, 431–437.

Liu, N., Zhu, Q.M., Wei, C.Y., Dykes, N.D., Irving, P.E., 1999. Impact damage detection in carbon fibre composites using neural networks and acoustic emission. Key Engng. Mater. 167, 43–54.

Luo, H., Hanagud, S., 1997. Dynamic learning rate neural networks training and composite structural damage detection. AIAA J. 35, 1522–1527.

Manson, R.L., Gunst, R.F., Hess, J.L., 1989. Statistical Design and Analysis of Experiments. Wiley, New York.

Masri, S.F., Ghassiakos, A.G., Caughey, T.K., 1996. Neural network approach to detection of changes in structural parameters. J. Engng Mech. 122, 350–360.

Riedmiller, M., Braun, H., 1993. A direct adaptive method for faster backpropagation learning: The RPROP algorithm. Proc. IEEE Int. Conf. Neural Networks. pp. 586–591.

Rhim, J., Lee, S.W., 1995. Neural network approach for damage detection and identification of structures. Comput. Mech. 16, 437–443.

Rogers, J.L., 1994. Simulating structural analysis with neural network. J. Comput. Civil Engng. 8, 252–265.

Vogl, T.P., Mangis, J.K., Rigler, A.K., Zink, W.T., Alkon, D.L., 1988. Accelerating the convergence of the back-propagation method. Biol Cyber 59, 257–263.

Wang, Y.Y., Lam, K.Y., Liu, G.R., 1998. Wave scattering of the interior vertical crack in plates and the detection of the crack. Engng. Frac. Mech. 59, 1–16.

Wu, X., Ghaboussi, J., Garrett, J.H., 1992. Use of neural networks in detection of structural damage. Comput. Struct. 42, 649–659.

Zhao, J., Ivan, J.N., DeWolf, J.T., 1998. Structural damage detection using artificial neural networks. J. Infrastr. Sys. 4, 93–101.